JOURNAL OF VIROLOGY, May 1993, p. 2689–2698
0022-538X/93/052689-10$02.00/0

Vol. 67, No. 5

Vaccinia Virus Morphogenesis Is Blocked by a Temperature-Sensitive Mutation in the I7 Gene That Encodes a Virion Component

EILEEN M. KANE AND STEWART SHUMAN*

Program in Molecular Biology, Sloan-Kettering Institute, New York, New York 10021

Received 18 December 1992/Accepted 28 January 1993

The *ts*16 mutation of vaccinia virus WR (R. C. Condit, A. Motyczka, and G. Spizz, Virology 128:429–443, 1983) has been mapped by marker rescue to the I7L open reading frame located within the genomic *Hin*dIII I DNA fragment. The I7 gene encodes a 423-amino-acid polypeptide. Thermolabile growth was attributed to an amino acid substitution, Pro-344→Leu, in the predicted I7 protein. A normal temporal pattern of viral protein synthesis was elicited in cells infected with *ts*16 at the nonpermissive temperature (40°C). Electron microscopy revealed a defect in virion assembly at 40°C. Morphogenesis was arrested at a stage subsequent to formation of spherical immature particles. Western immunoblot analysis with antiserum directed against the I7 polypeptide demonstrated an immunoreactive 47-kDa polypeptide accumulating during the late phase of synchronous vaccinia virus infection. Immunoblotting of extracts of wild-type virions showed that the I7 protein is encapsidated within the virus core. The I7 polypeptide displays amino acid sequence similarity to the type II DNA topoisomerase of *Saccharomyces cerevisiae*.

The genes essential for the replication of vaccinia virus in cultured cells have been identified classically through study of conditionally lethal (temperature-sensitive [*ts*]) mutations in viruses (7–9, 11, 14, 44). Condit and colleagues (7, 8, 44) have collected 65 *ts* mutants comprising 31 complementation groups. Four phenotypes, based on patterns of macromolecular synthesis under nonpermissive growth conditions, have been described; these are (i) DNA replication negative, (ii) abortive late protein synthesis, (iii) defective late protein synthesis, and (iv) "normal." Normal mutants exhibit a wild-type (WT) pattern of DNA replication and protein synthesis at the nonpermissive temperature.

The normal phenotype suggests mutation of a viral gene whose protein product might either participate in virion morphogenesis or be essential for establishment of the next round of infection (e.g., during virus penetration or the synthesis of early mRNAs by the virion-encapsidated RNA polymerase). The mutations in several normal mutants from the Condit collection have been mapped by marker rescue to individual viral genes. In some instances, the gene product has been identified as an enzymatic component of the virus particle with a presumptive role in early transcription. For example, a thermolabile mutation in the H4 gene (encoding a 94-kDa component of the virion RNA polymerase [1, 23]) results in the production of progeny virions that are morphologically normal (as determined by electron microscopy) but noninfectious (23). *ts* mutations in the I8 gene (which encodes a virion-associated nucleoside triphosphate-dependent RNA helicase [38]) also result in the production of noninfectious mature virus particles (16). Another normal-mutant mutation maps to gene D6R, which encodes the 73-kDa subunit of VETF, an early transcription factor required for initiation of early mRNA synthesis by the virion RNA polymerase (5, 37). The Dales collection of vaccinia virus mutants includes four *ts* isolates that produce microscopically normal noninfectious progeny at the nonpermissive temperature (9); these mutations, when mapped, may also define proteins that participate in early mRNA synthesis.

Normal thermosensitive mutations affecting viral structural proteins can result in defective virus assembly. The biochemical studies of Dyster and Niles (13) indicate that morphogenesis is interrupted when viruses mutated in gene D2 or D3 (encoding 17-kDa and 27-kDa virion core proteins, respectively [13, 29]) are grown at the nonpermissive temperature; the nature of the morphogenetic block has not been evaluated microscopically. Normal thermosensitive mutations also map to gene D13, which encodes a 65-kDa protein required for formation of the immature virus envelope (2, 25, 37, 43, 48). Dales and coworkers have documented, by electron microscopy, altered patterns of morphogenesis when the *ts* vaccinia virus mutants from their collection were grown under nonpermissive conditions (9, 15). Although as many as 17 phenotypic categories, based on the types of viral structures accumulating at 40°C, were described, the mutations responsible have not been mapped as yet to individual viral genes. Recently, specific gene products involved in vaccinia virus morphogenesis have been identified through the creation of "null" alleles, e.g., via conditional repression of individual transcription units (4, 12, 32, 46–48). This approach has been especially fruitful in defining proteins essential for virion envelopment and extracellular egress (4, 12, 32, 36, 48).

We now report that the mutation in the *ts*16 mutant of vaccinia virus WR, isolated originally by Condit et al. and classified as normal with respect to viral DNA and protein synthesis (7, 8), maps to the I7 gene, encoding a 47-kDa component of the mature virus particle. We find that the failure to produce infectious virions at the nonpermissive temperature is caused by a specific block to virion morphogenesis during the transition from spherical immature particle to mature intracellular virion.

* Corresponding author.

MATERIALS AND METHODS

Cells and viruses. BSC40 cells were maintained in Dulbecco's modified Eagle's medium (DME) supplemented with 5% fetal calf serum (FCS). Wild-type vaccinia virus WR was propagated in BSC40 cells grown at 37°C. Vaccinia virus mutant *ts*16 was kindly provided by R. Condit, University of Florida. Mutant virus was subjected to two rounds of plaque purification in BSC40 cells grown at 31°C (permissive temperature) and then amplified in monolayer cultures at 31°C. The thermolability of mutant virus stocks was verified by comparative titration on BSC40 cells at 31 and 40°C (nonpermissive temperature).

One-step growth. Confluent monolayers of BSC40 cells (35-mm dishes) maintained at either 31 or 40°C were infected with either WT or mutant virus at a multiplicity of infection (MOI) of 5. The inoculum was removed after 30 min, and the cells were washed once with medium and then overlaid with fresh DME–5% FCS. Infected cells were harvested at various times postinfection by scraping the monolayer with a Teflon policeman. Cells were pelleted in a clinical centrifuge and then resuspended in 1 ml of DME. The suspension was subjected to three cycles of freezing and thawing, followed by three 30-s bursts of sonication. The titer was determined by serial 10-fold dilution of virus onto BSC40 cells grown at 31°C.

Metabolic labeling. Confluent BSC40 monolayers were infected with *ts*16 virus at an MOI of 10 at 31 and 40°C. At various times postinfection, the medium was removed, and the cells were washed with methionine-free DME and then overlaid with methionine-free DME containing 30 μCi of [^{35}S]methionine (>800 Ci/mmol) per ml for 30 min. This medium was removed, and the cells were lysed in situ by the addition of 0.15 ml of a solution containing 0.065 M Tris-HCl (pH 6.8), 2% sodium dodecyl sulfate (SDS), 5% β-mercaptoethanol, and 10% glycerol. Lysates were stored at −20°C. Samples (25-μl aliquots) were heated at 100°C for 5 min and then electrophoresed through a 12% polyacrylamide gel containing 0.1% SDS. Radiolabeled polypeptides were visualized by autoradiographic exposure of the dried gel.

Plasmids and molecular cloning. Plasmid pHindI, containing the 6.5-kb *Hin*dIII I restriction fragment of vaccinia virus WR (35) cloned into pUC13, was kindly supplied by M. Merchlinsky, National Institutes of Health. Subclones of the I fragment deleted unidirectionally from the left end were generated by cleaving pHindI with endonuclease *Pst*I or *Sal*I; these endonucleases cut at sites in the pUC polylinker and in the viral DNA insert. Digestion products were circularized by incubation with T4 DNA ligase, and the reaction products were transformed into *Escherichia coli* JM109. Plasmids pPH and pSH (named according to the restriction sites at the borders of the viral insert; see Fig. 1) were prepared by alkaline lysis and CsCl equilibrium centrifugation.

A plasmid containing only the I7 open reading frame (ORF) (35) was generated as follows. Oligonucleotide primers complementary to the 5′ and 3′ ends of the I7 ORF and containing restriction sites for *Nde*I and *Bgl*II, respectively, were used to amplify the I7 gene from the pHindI plasmid. Polymerase chain reaction was carried out with a GeneAmp reagent kit (Perkin Elmer Cetus). Polymerase chain reaction products were gel purified and cleaved with endonucleases *Nde*I and *Bgl*II. This I7-containing DNA was then inserted into plasmid pET3c (34) which had been digested with *Nde*I and *Bam*HI to generate plasmid pET-I7.

The genomic *Hin*dIII I fragment of mutant virus *ts*16 was gel purified from a *Hin*dIII digest of cytoplasmic DNA from BSC40 cells infected with *ts*16 at the permissive temperature; this fragment was inserted into pUC19 that had been cleaved with *Hin*dIII. Plasmid DNA was isolated as described above.

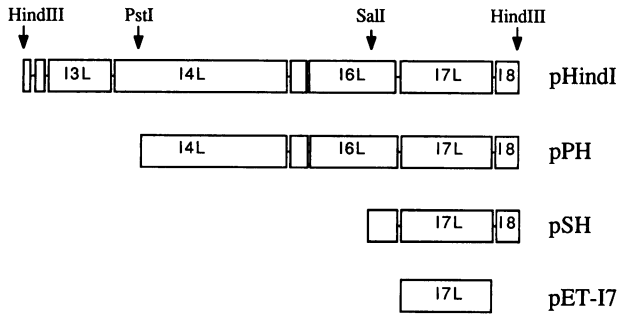

FIG. 1. Map of the genomic *Hin*dIII I fragment and subfragments used for marker rescue. Plasmid pHindI contains the full 6.5-kb *Hin*dIII I fragment cloned into pUC13. A physical and genetic map of the viral DNA insert is shown. *Hin*dIII restriction sites defining the borders of the viral DNA and internal sites for *Pst*I and *Sal*I used in subcloning are indicated by vertical arrows. Protein-encoding regions of the I fragment (illustrated as boxed segments) are distinguished from noncoding regions (intervening line segments). Genes are named according to the conventional poxvirus ORF notation (35). The letters R (right) and L (left) in the ORF nomenclature refer to the direction of transcription of the gene. pPH and pSH contain subregions of the H fragment extending from the right *Hin*dIII site to either the *Pst*I site (pPH) or the *Sal*I site (pSH). pET-I7 contains only the I7 ORF.

Marker rescue. Confluent BSC40 cell monolayers (35-mm dishes) were infected with virus at an MOI of 5 at 31°C. The inoculum was removed after 30 min, and the cells were washed once with medium and overlaid with DME–5% FCS. After 30 min, cells were dislodged from the monolayer by treatment with 1 ml of 0.05% trypsin–0.53 mM EDTA. Suspended cells were mixed with 4 ml of DME and recovered by centrifugation for 5 min at 4°C in a clinical centrifuge. The pellet was washed with 0.5 ml of HBS (20 mM HEPES [*N*-2-hydroxyethylpiperazine-*N*′-2-ethanesulfonic acid, pH 7.0], 150 mM NaCl, 0.7 mM Na_2HPO_4, 5 mM KCl, 6 mM dextrose) and centrifuged as before. The pellet was resuspended in 1 ml of cold HBS by pipetting and kept on ice. An aliquot (0.8 ml) of the suspension was transferred to a chilled Bio-Rad 0.4-cm electrode gap cuvette. Plasmid DNA (10 μg) was added to the cuvette and mixed by pipetting, and the cuvette was chilled on ice for 10 min. The cuvette was pulsed at 200 V (capacitance, 960 μF) in a Bio-Rad Gene Pulser equipped with a Bio-Rad Capacitance Extender and then kept on ice for 10 min. The suspension was diluted into 8 ml of medium at room temperature. An aliquot (3 ml) was then applied to a confluent monolayer of BSC40 cells (35-mm well) maintained at 40°C. After 2 days of incubation at 40°C, the cells were stained with 0.1% crystal violet in order to visualize plaques formed from infectious centers.

DNA sequence analysis. Plasmid DNA was sequenced by the dideoxy nucleotide chain termination method. A T7 DNA polymerase-based sequencing kit (Sequenase, Version 2.0) was used according to the protocols supplied by the manufacturer (United States Biochemical).

Electron microscopy. Confluent BSC40 cell monolayers (35-mm dishes) maintained at either 31 or 40°C were infected with virus at an MOI of 5. The inoculum was removed after

1 h, and the cells were washed twice with medium and then overlaid with fresh DME–5% FCS. At 24 or 48 h postinfection, the cells were dislodged by scraping and then spun in a clinical centrifuge at 4°C. The supernatant was removed, and the cell pellet was placed immediately on ice. Cells were fixed initially in 2.5% glutaraldehyde and then in 2% osmium tetroxide. Specimens were dehydrated and then embedded in epoxy resin (Polybed 812). Thin sections were stained with uranyl acetate and lead citrate for visualization in a JEOL 1200 CX transmission electron microscope.

Anti-I7 serum. The protein used for immunization was obtained from the insoluble fraction of lysates of bacteria that had been induced to overexpress the I7 ORF. Insoluble polypeptides were resolved by preparative SDS-polyacrylamide gel electrophoresis (PAGE). The I7 polypeptide was eluted from an excised gel slice. Immunization (with approximately 200 μg of antigen per rabbit) was performed at Pocono Hill Rabbit Farm, Canadensis, Pa. The specificity of preimmune and immune sera was determined by Western immunoblotting against appropriate test antigens. Protein samples were electrophoresed through a 10% polyacrylamide gel containing 0.1% SDS, and polypeptides were transferred electrophoretically to a nitrocellulose membrane. Western blotting was performed as described before (23).

Virion extracts. Vaccinia virions (1,800 A_{260} units), grown in HeLa suspension cultures and purified by sucrose gradient sedimentation, were fractionated as described before (39). The envelope fraction (9 ml) refers to material solubilized by treatment of virions with 50 mM dithiothreitol and 0.5% Nonidet P-40 (NP-40). All subsequent steps were performed at 4°C. The virus core was extracted with buffer containing 0.1% sodium deoxycholate (DOC) in 0.3 M Tris-HCl (pH 8.0)–50 mM dithiothreitol–0.25 M NaCl. Material solubilized by this treatment is referred to as the DOC-1 fraction (9 ml). The 0.1% DOC-insoluble material was reextracted first with buffer A (39), containing 0.2 M NaCl and 0.05% NP-40 (yielding the NP-1 fraction; 6 ml), and then with 0.2% DOC in buffer A. Protein rendered soluble by 0.2% DOC (DOC-2 fraction; 5 ml) was separated by centrifugation from the residual insoluble material (pellet fraction). This pellet was resuspended in 5 ml of 0.2 M NaCl in buffer A.

RESULTS

Growth characteristics of mutant viruses. Stocks of *ts*16 prepared at the permissive temperature (31°C) were tested for their ability to form plaques at both 31 and 40°C in BSC40 cells. The efficiency of plaque formation was reduced by >100,000-fold at the nonpermissive temperature (data not shown). In contrast, plaque formation by WT virus was equivalent at 31 and 40°C.

In order to determine whether defective plaque formation was caused by a failure of the *ts* virus to replicate or to spread, one-step growth experiments were performed at both 31 and 40°C. Cells were harvested at 2, 24, and 48 h after infection, and the production of infectious virus was assayed by titration at 31°C (Table 1). The yield of *ts*16 progeny at 48 h at the permissive temperature (3×10^8 PFU) reflected a burst size of >100 PFU/cell. No increase in the titer over background was observed when infection was performed at the nonpermissive temperature. Growth of WT virus did not vary with temperature (23). Thus, the plaque phenotype of the *ts*16 mutants was clearly attributable to a profound thermosensitive defect in viral replication.

The patterns of viral protein synthesis at the permissive and nonpermissive temperatures were analyzed by pulse-labeling synchronously infected cells with [^{35}S]methionine over a 24-h time course postinfection. The normal temporal pattern of vaccinia virus gene expression was observed in cells infected with *ts*16 at 31°C, i.e., appearance of novel early polypeptides at 2 to 4 h postinfection, transition to synthesis of distinctive late proteins by 8 h, and shutoff of host protein synthesis late in infection (data not shown). Identical transitions were observed in cells infected with *ts*16 virus at 40°C (data not shown). Thus, *ts*16 displayed a "normal" phenotype, as reported originally (7, 8).

TABLE 1. One-step growth of *ts*16 mutant virus at the permissive and nonpermissive temperatures[a]

Temp (°C)	Titer (PFU/ml) at time postinfection:		
	2 h	24 h	48 h
31	9×10^5	8×10^7	3×10^8
40	4×10^4	4×10^5	4×10^5

[a] BSC40 cells maintained at 31 or 40°C were infected with *ts*16 virus at an MOI of 5. At the indicated times postinfection, cells were harvested and titered by serial 10-fold dilution onto BSC40 cells at 31°C. Plaques were visualized at 2 days postinfection by staining with 0.1% crystal violet in 20% ethanol.

Marker rescue. It was shown previously that *ts*16 could be restored to temperature-independent growth by marker rescue with a plasmid containing the entire *Hin*dIII I genomic fragment derived from WT virus (44). An annotated map of the 6.5-kb I fragment is shown in Fig. 1. We have refined the analysis by using an electroporation-based protocol for DNA-mediated marker rescue. Cells infected with *ts*16 were electroporated with plasmid DNA (30) and plated onto uninfected-cell monolayers maintained at the nonpermissive temperature. Successful marker rescue yields recombinant WT progeny from individual electroporated cells that were seeded onto the fresh monolayer; this was manifested as a plaque arising from each infectious center. No infectious centers were observed when monolayers were seeded with uninfected cells that had been electroporated without added DNA (Fig. 2B, no virus) or with virus-infected cells that had been electroporated without added DNA (Fig. 2, no DNA). Robust marker rescue was achieved by electroporation with the pHindI plasmid, containing the entire WT *Hin*dIII I fragment, but not with plasmid pHindH, containing the 8.6-kb WT *Hin*dIII H fragment (Fig. 2A). Comparable rescue was obtained with the I fragment subclones pPH and pSH (Fig. 2B). These results localized the *ts* mutations to a segment between the *Sal*I and *Hin*dIII restriction sites that included the entire I7L ORF, the amino terminus of the I6L ORF, and an amino-terminal portion of the I8R ORF. Plasmid pET-I7, containing no vaccinia virus sequence extraneous to the I7 ORF, was able to rescue *ts*16 (Fig. 2B). We therefore concluded that the genetic lesion of *ts*16 occurred in the I7 gene.

Sequence analysis of the I7 gene. The I7 gene of the WR strain of vaccinia virus (35) encodes a protein of 423 amino acids, with a predicted molecular mass of 49 kDa. In order to fine-map the *ts*16 mutation, the genomic *Hin*dIII I fragment of *ts*16 viral DNA was isolated from virus-infected cells and cloned into a pUC plasmid vector. The nucleotide sequence of the I7 gene of this *ts*16 plasmid diverged from that of the wild-type I7 gene at a single position. A codon alteration (CCT→CTT) resulted in a predicted Pro to Leu change at residue 344 of the I7 polypeptide.

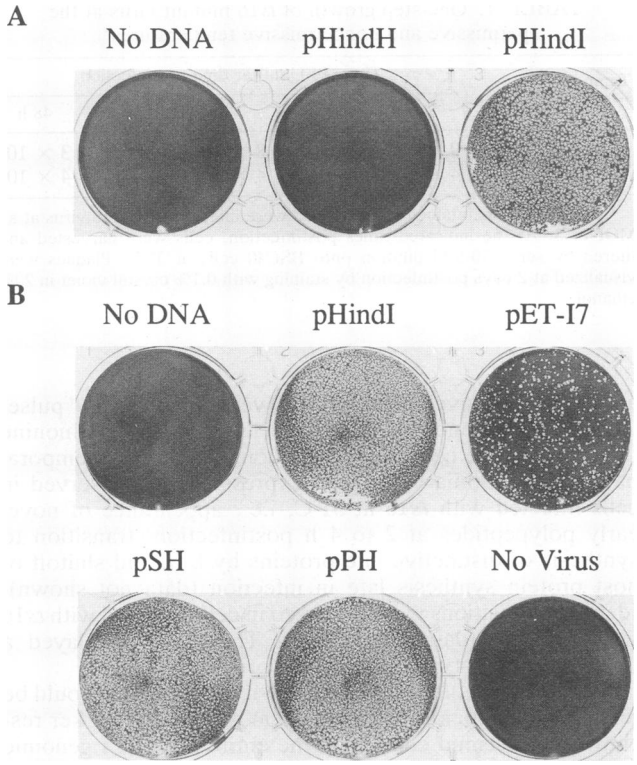

FIG. 2. Marker rescue of *ts*16. Electroporation-based marker rescue with supercoiled plasmid DNAs (23, 30) was performed as described in the text. Photographs of the stained monolayers from two experiments are shown in A and B. The plasmid tested is indicated above the well. pHindH contains the entire 8.6-kb genomic *Hin*dIII H fragment inserted in pUC13 (33). The no-virus control entailed seeding the monolayers with uninfected BSC40 cells that had been electroporated without added DNA.

```
  RYTEARMSKI (B.subtilis gyrA)
  :::.  .:::
MERYTDLVISKIPELGFTNLLCHIYSLAGLCSNIDVSKFLTNCNGYVVEK  I-7
                              ::         :   .  : .:
                        (149)LCNIFSTEFILETADLNVGGK  TOP2

YDKSTTAGKVSCIPIGMMLELVESGHLSRPNSSDELDQKKELTDELKTRY  I-7
:          : :   .          .     .:  .  .  ::
YVQKWENNMSICHP-PKITSYKKGPSYTKVTFKPDLT-RFGM-KELDNDI  TOP2

HSIYDVFELPTSIPLAYFFKPRLREKVSKAIDFSQMDLKIDDLSRKGIHT  I-7
  .  :...  :. .  ..  .   :.    .. .. ::  .  .. .
LGVMRVYDINSGVRINVYLNGK-SLKIRNFKNYVELYLKSLE-KKRQLDN  TOP2
    RR       D

GENPKVVKMKIEPERGAWMSNRSIKNLVSQFAYGSEVDYIGQFDMRFLNS  I-7
::.    :  :      .. :: .   ::.  .  .. ..       .
GEDG-AAKSDIPTILYERINNREVAFAVSDISF-QQISFVNSIATT-MGG  TOP2
                    W

LAIHEKFDAFMNKHILSYILKDKIKSSTSRFVMFGFCYLSHWKCVIYDKK  I-7
  ..   :  . : : : ::: : : :   : .    ..    :.:
THVNYITDQIVKK-I-SEILKKKKKKSVKSFQIKNNMFIFI-NCLI(358) TOP2

QCLVSFYDSGGNIPTEFHHYNNFYFYSFSDGFNTNHKHSVLDNTNCDIDV  I-7
                                          L
LFRFFECTFGAKIGCINVEVNQLLESECGMFISLFMILCTRTPPKSFKSL  I-7

KKVYTFFKFLADKKMTLFKSILFNLHDLSLDITETDNAGLKEYKRMEKWT  I7

KKSINVICDKLTTKLNRIVNDDE                              I7
```

FIG. 3. Sequence similarity between the I7 protein and DNA topoisomerase II. Computer-assisted sequence alignment between the vaccinia virus I7 protein (strain WR) and the *S. cerevisiae* DNA topoisomerase II (TOP2) is shown. Identical amino acids are indicated by a colon; conserved amino acids are denoted by a single dot. The entire I7 sequence is displayed continuously from residues 1 to 423; the region of alignment to TOP2 extends from amino acid residues 149 to 358 of the yeast polypeptide (19). Single-residue discontinuities in the TOP2 sequence are shown as dashed lines (—) for gaps or, in the case of insertions, as extra amino acid residues below the TOP2 sequence. A short segment of similarity between the I7 protein (residues 3 to 12) and the active site of *B. subtilis* DNA gyrase (located within the GyrA polypeptide [27]) is also shown. The sequence of the I7 protein from the WR strain (35) differs at two positions from the I7 protein of the Copenhagen strain (20); these positions are indicated by underlined residues. The *ts*16 mutation P(344)→L is indicated in boldface above the sequence.

A search of the GenBank data base with the I7 amino acid sequence and MacVector software (IBI) turned up numerous alignments. One computer-assisted alignment of significance (optimized score, 266) was to the G1L ORF of the *Amsacta moorei* entomopoxvirus (21). The insect poxvirus gene encodes a 464-amino-acid polypeptide that shows 24% identity with the vaccinia virus I7 protein over a 335-amino-acid region. This sequence similarity has been reported previously by Hall and Moyer (21). The function of the G1 gene during entomopoxvirus replication is unknown. Another alignment (score, 115) of great potential interest was to the type II DNA topoisomerase of the yeast *Saccharomyces cerevisiae* (Fig. 3). The two proteins display 17% sequence identity plus 20% conserved residues over a 217-amino-acid segment of the I7 protein. The segment of topoisomerase II to which I7 is aligned derives from the amino portion of the TOP2 protein (19); this region of TOP2 is homologous to the GyrB subunit of bacterial type II topoisomerases. Visual inspection also revealed a short segment of sequence conservation between the amino terminus of the I7 protein and the active site of *Bacillus subtilis* DNA gyrase (27), located within the GyrA enzyme subunit (Fig. 3). The possible significance of the similarity to topoisomerase II is considered below.

Expression of the I7 protein. Heterologous expression of the I7 ORF in bacteria was accomplished by using a T7 RNA polymerase-based expression system (34). Bacteria carrying the pET-I7 plasmid were induced to express the viral gene by infection with bacteriophage λCE6 as described before (40). This resulted in the time-dependent accumulation of a prominent 45-kDa polypeptide that was recovered exclusively in the insoluble fraction of crude bacterial lysates (data not shown). This polypeptide was purified from the insoluble fraction and used to prepare rabbit antiserum against the I7 protein.

To examine the expression of the I7 gene product during vaccinia virus infection of cultured cells, BSC40 monolayers were infected synchronously with wild-type vaccinia virus and harvested at various times postinfection. Polypeptides were resolved by SDS-PAGE and transferred to nitrocellulose membranes that were then probed by Western blotting with anti-I7 serum (Fig. 4). No immunoreactivity was seen with polypeptides present in uninfected cells (time zero) or during the early stage of the infectious cycle (2 h). An immunoreactive species of 47 kDa appeared at late times (8 h) and continued to accumulate at 16 and 24 h postinfection.

The expression of the I7 protein was examined in cells synchronously infected with *ts*16 virus at the permissive and

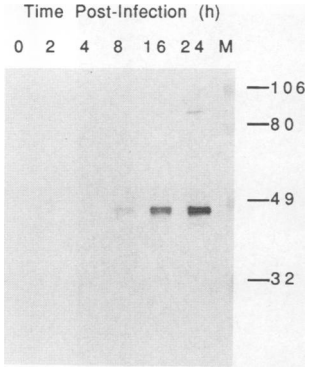

FIG. 4. Expression of the I7 protein during WT vaccinia virus infection. BSC40 monolayers were infected at 37°C with WT vaccinia virus at an MOI of 10. At the indicated times postinfection, the cells were lysed in situ as described in the text for the metabolic labeling experiments. Time zero refers to uninfected cells. Lysates (5-μl aliquots) were heated at 100°C for 5 min and then electrophoresed through a 10% polyacrylamide gel containing 0.1% SDS. Polypeptides were transferred electrophoretically to a nitrocellulose membrane that was then blocked in TBST buffer (10 mM Tris-HCl [pH 8], 150 mM NaCl, 0.05% Tween-20) containing 1% bovine serum albumin. Membranes were incubated for 30 min at room temperature with rabbit anti-I7 serum diluted 1:1,000 in TBST. After removal of serum and washing with TBST, bound antibodies were localized by incubation with immunoglobulin conjugated with alkaline phosphatase by using a ProtoBlot AP system (Promega). The positions and sizes (in kilodaltons) of coelectrophoresed prestained protein markers (lane M) are indicated at the right.

nonpermissive temperatures (Fig. 5). Western blots again showed the appearance of an immunoreactive 47-kDa polypeptide after virus infection. The accumulation of I7 protein at both growth temperatures suggested that the failure to produce infectious progeny at the nonpermissive temperature was not caused by a complete lack of the I7 gene product (e.g., because of increased turnover of the mutated polypeptide, as noted for other vaccinia virus *ts* mutants [13, 31]), but was an effect of the amino acid substitution on I7 protein function.

Electron microscopy. Viral structures typical of the normal morphogenetic pathway were apparent in electron micrographs of BSC40 cells infected with *ts*16 at the permissive temperature (Fig. 6). The earliest of these are crescent-shaped spicule-coated viral membranes that enclose granular material. These membranes are seen surrounding centers of electron-dense viroplasm (Fig. 6, arrow at lower left). Spherical immature viral particles are formed upon closure of the membrane around the granular material (Fig. 6, arrowheads). These immature particles evolve into mature brick-shaped virions, clusters of which are evident (Fig. 6, m). The characteristic biconcave core and two flanking lateral bodies contained within a viral membrane were apparent in the micrograph shown in Fig. 6 and in high-magnification views that are not shown. Structural intermediates between immature and mature particles, including the closed immature particle with nucleoid, were also detected. These mature and immature *ts*16 particles were indistinguishable microscopically from those observed in cells infected with WT virus (not shown).

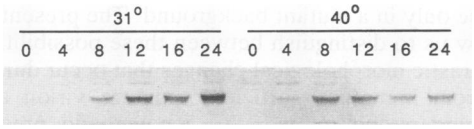

FIG. 5. Expression of the I7 protein during infection with *ts*16 mutant virus. BSC40 monolayers were infected at either 31 or 40°C with *ts*16 virus at an MOI of 10. At the indicated times (hours) postinfection, the cells were lysed in situ. Time zero refers to uninfected cells. Aliquots (10 μl) of each lysate were electrophoresed through a 10% polyacrylamide gel containing 0.1% SDS. Polypeptides were transferred electrophoretically to a nitrocellulose membrane, which was probed with anti-I7 serum (1:1,000 dilution) as described in the legend to Fig. 4. The region of the blot containing the immunoreactive I7 polypeptide is shown.

No mature progeny virions could be detected in the cytoplasm of cells infected with *ts*16 at the nonpermissive temperature, although viral membranes and spherical immature particles were encountered (Fig. 7; other data not shown). Many of the spherical immature particles seen at 48 h were obviously unusual. The diffuse granular material within the sphere had condensed asymmetrically, so that one side of the particle appeared empty (Fig. 7, arrow). A higher-magnification view of these forms (which we dub half-moons) is shown in Fig. 8. There is often a sharp demarcation between the empty and full sides of these particles. Some of the particles contain a residual electron-dense body on the transparent side (Fig. 8, arrows) that appears unconnected to the full side of the half-moon. Other particles contain round or oval densities at the junction between the full and empty halves (e.g., particle denoted by arrowhead in Fig. 8A). Examination of nonpermissively infected cells at 24 h postinfection revealed numerous closed immature particles with a nucleoid as well as the asymmetric half-moon forms (not shown). These findings indicate that the I7 gene product plays an essential role in virion morphogenesis, presumably during the extensive structural transition from immature spherical particle to mature intracellular virion. The origins of the unusual *ts*16 structures that accumulate at the nonpermissive temperature are considered in the Discussion.

Localization of the I7 protein in virion cores. In order to examine whether the I7 protein is a virion component, anti-I7 serum was tested in Western blotting experiments against extracts of highly purified virus particles. The polypeptide compositions of the virion envelope fraction, detergent extracts of virion cores (extracted serially with 0.1% DOC, 0.05% NP-40, and 0.2% DOC), and the insoluble pellet fraction were examined by SDS-PAGE in order to monitor the integrity of the extraction procedure (Fig. 9A). Virion proteins were partitioned in characteristic fashion; for example, the major virion polypeptides 4a and 4b were found exclusively in the insoluble pellet. Distinct subsets of viral proteins were released from cores by treatment with 0.1% DOC and 0.2% DOC, whereas the intervening NP-40 wash yielded a set of polypeptides similar to that released by 0.1% DOC. Western blotting revealed an I7-immunoreactive polypeptide of 47 kDa that was present in the DOC-1 extract and NP-40 wash (NP-1) of virus cores but virtually absent from the envelope fraction (Fig. 9B). The size of this protein was the same as that of the I7 gene product that accumulated late in infection. No reactive protein of this size was detected by preimmune serum. The I7 protein was more abundant in the 0.1% DOC extract than in the 0.2% DOC fraction. This pattern of partitioning during extraction resembles that of the virion-associated ATPases and contrasts with that of the vaccinia virus RNA polymerase, which is recovered predominantly in the DOC-2 fraction (23) (data

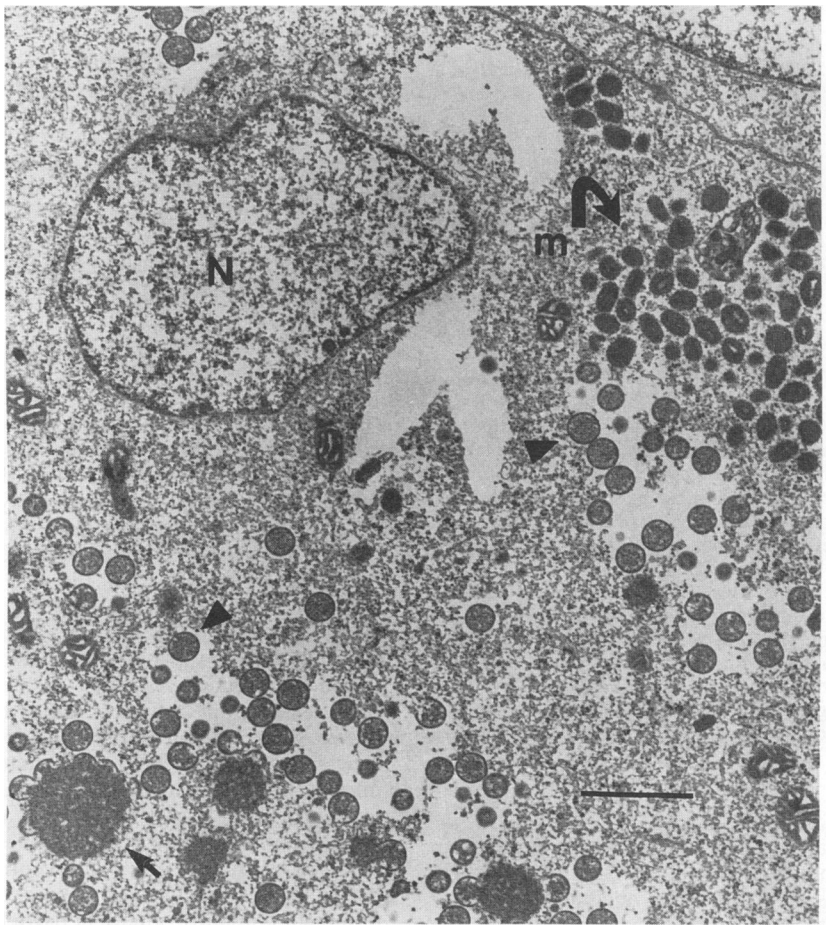

FIG. 6. Electron microscopic analysis of *ts*16 morphogenesis at the permissive temperature. Cells infected with *ts*16 virus at 31°C were harvested at 48 h postinfection and analyzed by electron microscopy. A representative micrograph (magnification, ×7,500) shows several stages of viral morphogenesis. Structures are indicated as follows: N, nucleus; m with curved arrow, clustered mature progeny virions; arrowheads, immature spherical particles; arrow, viroplasm with surrounding viral membrane crescents. Bar, 1 μm.

not shown). Residual I7 protein was also detected in the insoluble pellet fraction (data not shown). These data indicated that the I7 protein is a component of the vaccinia virus core.

DISCUSSION

The mutation responsible for thermosensitive growth of vaccinia virus *ts*16 has been mapped by marker rescue to the I7L ORF. The I7 gene, encoding a 423-amino-acid polypeptide, is expressed late in infection. The 5′ end of the I7 late RNA had been mapped by S1 nuclease protection to within the sequence TAAATG immediately preceding the translational start site of the I7 ORF (35). This motif is essential for the function of a vaccinia virus late promoter (10). The time course of accumulation of immunoreactive I7 protein during infection with wild-type virus was consistent with the expression of I7 at late times. The I7 gene of the *ts*16 virus contained a missense mutation.

Condit et al. (7, 8) had already assigned *ts*16 to the class of mutants displaying normal macromolecular synthetic patterns at the nonpermissive temperature, a result that we have confirmed herein and extended by examination of the protein-synthetic pattern over a period of 24 h postinfection. Electron microscopy of *ts*16-infected cells now reveals that assembly of normal progeny virions could not occur at the nonpermissive temperature. Morphogenesis was arrested at a stage subsequent to the formation of spherical immature particles. The accumulation of unusual viral particles, which we have termed half-moons, was a characteristic microscopic finding. It is conceivable that the half-moon forms are transient intermediates during normal morphogenesis, whose accumulation during *ts*16 infection was caused by a failure to execute the next step in the assembly pathway. Alternatively, the half-moons may be aberrant structures that arise only in a mutant background. The present data do not allow us to distinguish between these possibilities.

The drastic morphological changes that occur during transition from immature particle to mature virion are very poorly understood (6, 26, 28). Known and presumptive events include condensation of the viral genome, recruitment and positioning of the transcription machinery (with attention to proper stoichiometry of encapsidated enzymes), proteolytic processing of major structural proteins, formation of the core and lateral bodies, and reorganization of the viral membranes. Although structural intermediates have been observed microscopically, these have not been correlated to a defined genetic or biochemical pathway. In the case of the *ts*16 mutant, initial formation of the nucleoid

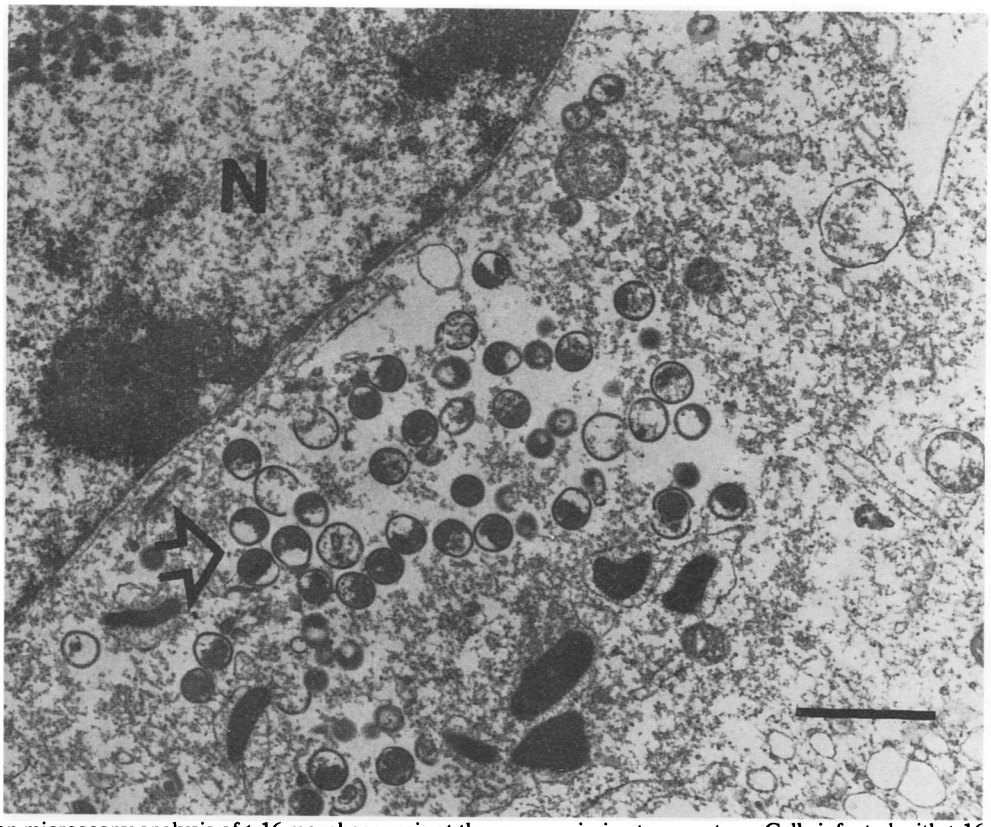

FIG. 7. Electron microscopy analysis of *ts*16 morphogenesis at the nonpermissive temperature. Cells infected with *ts*16 virus at 40°C were harvested at 48 h postinfection and viewed by electron microscopy at magnification ×5,000. N, nucleus; open arrow, unusual immature spherical particles (half-moons). Bar, 1 μm.

within the closed immature particle occurred at the nonpermissive temperature, but the core and lateral bodies did not evolve fully. Rather, the I7 mutation caused a profound structural asymmetry during internal maturation of the particle. This effect cannot be attributed to an absence of the I7 protein at 40°C, as indicated by the Western blot data. Our finding that the I7 protein is a normal component of the mature virion core suggests that I7 either is contained within the immature spherical particles or is encapsidated during subsequent maturation steps. Whether it is actually present within the *ts*16 mutant immature particles at 40°C remains an open question.

The microscopic appearance of the *ts*16 mutant is vaguely reminiscent of the category K morphological aberrations described by Dales et al. for three members of their *ts* mutant collection (9). These mutants accumulate "immature particles with nucleoids, but lacking internal dense material" (9). Indeed, the spherical particles with "partially lucent" centers in the published micrograph (9) bear some resemblance to the half-moons observed by us. Physical mapping and complementation analysis would clarify whether any of the mutations in the Dales collection of mutants are allelic with that of *ts*16 and might reveal genes other than I7 that act at or near a common point in the assembly pathway.

The amino acid sequence similarity between the I7 protein and yeast DNA topoisomerase II is intriguing in light of the morphogenetic phenotype. Eukaryotic topoisomerase II has been shown to be a major structural component of the nuclear matrix or scaffold (3). The DNA sequence elements that are in contact with the scaffold (so-called SARs) conform to the preferred DNA binding and cleavage sites for topoisomerase II (18), suggesting that topoisomerase II has a prominent role in the organization of the genome within the nucleus (beyond its essential function in chromosome partitioning during mitosis). It is conceivable that the I7 protein serves a loosely analogous role in the organization of the vaccinia virus genome within the core. That a poxvirus should encode a protein with similarity to topoisomerase II is not entirely surprising, as vaccinia virus is known to encode a type I DNA topoisomerase with structural and functional similarity to the nuclear type I counterpart (42). The vaccinia virus topoisomerase I is packaged in the virion and is essential for virus replication in vivo (41). A gene homologous to topoisomerase II has been identified in African swine fever virus, a eukaryotic DNA virus that strongly resembles the poxviruses in genome structure and the encapsidation of virus-encoded enzymes required for synthesis of early mRNAs (17). Does the vaccinia virus I7 protein actually have topoisomerase II activity, or is it even capable of binding to DNA? These are critical issues that will be addressed once the protein has been purified from virion extracts.

Little is known about the spatial configuration of the genome within the virion, i.e., whether it is partitioned into topological or functional domains (perhaps along boundaries dictated by transcription units), whether the DNA is attached to any kind of matrix, etc. Experiments involving controlled disruption of isolated virions suggest that the DNA exists as a nucleoprotein associated with two major polypeptides of 27 and 13 kDa (22). Two viral DNA-binding

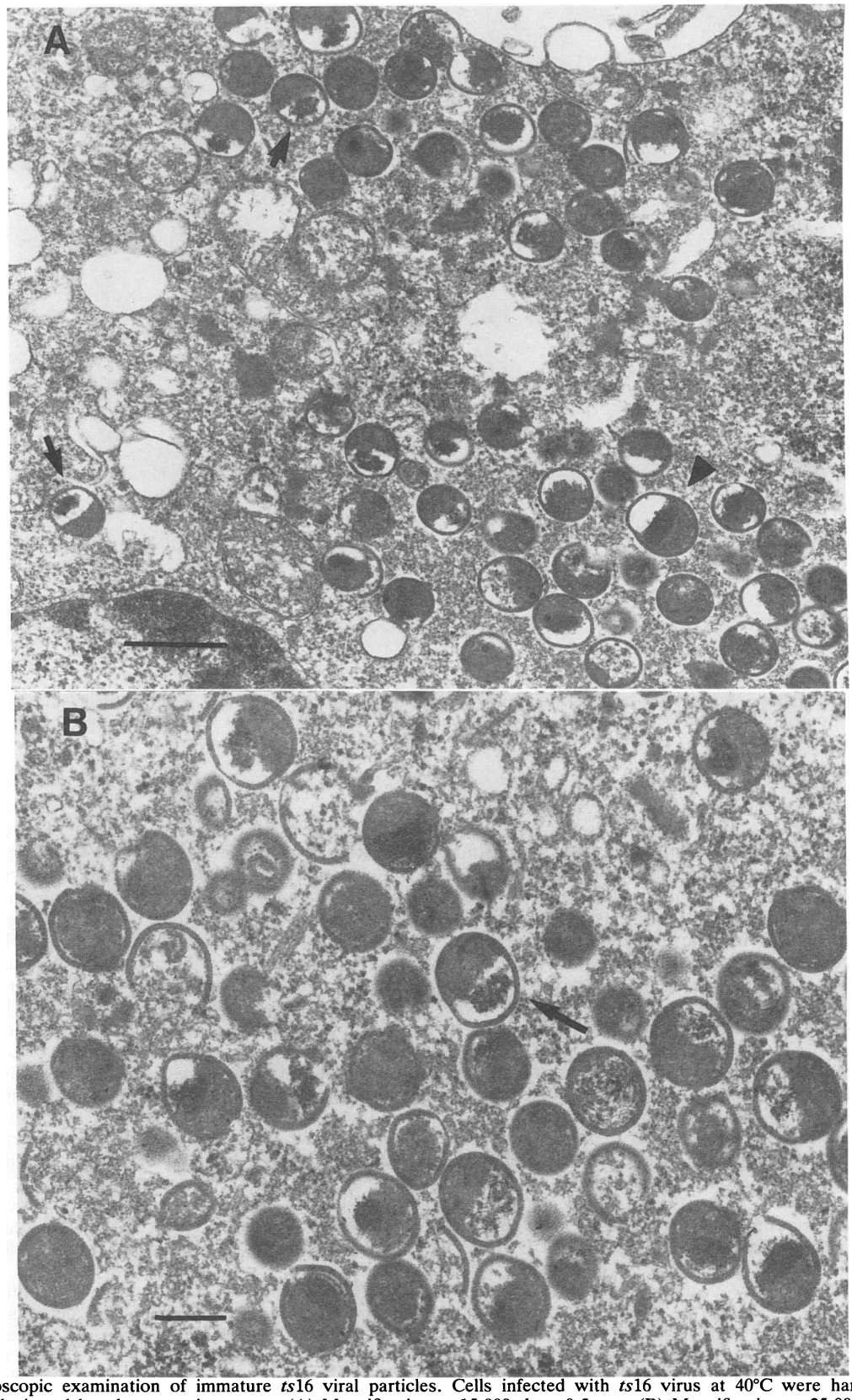

FIG. 8. Microscopic examination of immature *ts*16 viral particles. Cells infected with *ts*16 virus at 40°C were harvested at 48 h postinfection and viewed by electron microscopy. (A) Magnification, ×15,000; bar, 0.5 μm. (B) Magnification, ×25,000; bar, 0.2 μm. Representative half-moon immature particles are indicated by arrows and arrowheads.

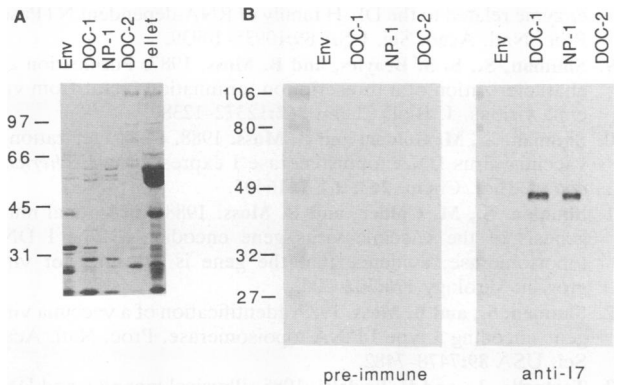

FIG. 9. Association of I7 protein with virus cores. (A) Extracts of purified WT virions were prepared as described in the text. Aliquots (10 μl of each fraction) were analyzed by electrophoresis through a 10% polyacrylamide gel containing 0.1% SDS. Polypeptides were visualized by staining with Coomassie blue. (B) Aliquots (5 μl of each fraction) were electrophoresed through a 10% polyacrylamide gel containing 0.1% SDS. Polypeptides were transferred to nitrocellulose membranes for immunoblotting with 1:4,000 dilutions of either preimmune or anti-I7 serum. The source of the protein fraction is indicated above each lane. The locations and sizes (in kilodaltons) of marker proteins are shown at the left of each panel.

proteins (DBPs), 25 and 11 kDa in size (and presumably identical to the nucleoprotein constituents just mentioned), have been purified from virion extracts (24, 45). Interestingly, conditional repression of the gene encoding the 11-kDa DBP results in a block to morphogenesis subsequent to the formation of immature spherical particles (46, 47). Electron micrographs of nonpermissively infected cells revealed immature particles with a nucleoid as well as accumulation of immature forms with aberrant internal structures (47). The aberrant particles generated by repression of the 11-kDa DBP were distinct in microscopic appearance from the half-moon forms found during growth of *ts*16 at the nonpermissive temperature. Nonetheless, we suspect that both the 11-kDa DBP and the I7 protein are requisite participants in a pathway of viral genome organization, disruption of which leads to arrest or alteration of the internal maturation of the spherical particle.

ACKNOWLEDGMENTS

We are indebted to Richard Condit for valuable advice and provision of mutant virus. Nina Lampen contributed expert assistance in electron microscopy.

This work was supported by NIH grants GM42498 and GM46330 and by ACS grant JFRA-274. S.S. is the recipient of a Pew Scholarship in the Biomedical Sciences.

REFERENCES

1. **Ahn, B., and B. Moss.** 1992. RNA polymerase-associated transcription specificity factor encoded by vaccinia virus. Proc. Natl. Acad. Sci. USA **89:**3536–3540.
2. **Baldick, C. J., and B. Moss.** 1987. Resistance of vaccinia virus to rifampin conferred by a single nucleotide substitution near the predicted amino terminus of a gene encoding an Mr 62,000 polypeptide. Virology **156:**138–145.
3. **Berrios, M., V. Osheroff, and P. A. Fisher.** 1985. In situ localization of DNA topoisomerase II, a major polypeptide component of the *Drosophila* nuclear matrix fraction. Proc. Natl. Acad. Sci. USA **82:**4142–4146.
4. **Blasco, R., and B. Moss.** 1991. Extracellular vaccinia virus formation and cell-to-cell virus transmission are prevented by deletion of the gene encoding the 37,000-dalton outer envelope protein. J. Virol. **65:**5910–5920.
5. **Broyles, S. B., and B. S. Fesler.** 1990. Vaccinia virus gene encoding a component of the viral early transcription factor. J. Virol. **64:**1523–1529.
6. **Buller, R. M. L., and G. J. Palumbo.** 1991. Poxvirus pathogenesis. Microbiol. Rev. **55:**80–122.
7. **Condit, R. C., and A. Motyczka.** 1981. Isolation and preliminary characterization of temperature-sensitive mutants of vaccinia virus. Virology **113:**224–241.
8. **Condit, R. C., A. Motyczka, and G. Spizz.** 1983. Isolation, characterization, and physical mapping of temperature-sensitive mutants of vaccinia virus. Virology **128:**429–443.
9. **Dales, S., V. Milanovitch, B. G. T. Pogo, S. B. Weintraub, T. Huima, S. Wilton, and G. McFadden.** 1978. Biogenesis of vaccinia: isolation of conditional lethal mutants and electron microscopic characterization of their phenotypically expressed defects. Virology **84:**403–428.
10. **Davison, A. J., and B. Moss.** 1989. Structure of vaccinia virus late promoters. J. Mol. Biol. **210:**771–784.
11. **Drillien, R., D. Spehner, and A. Kirn.** 1982. Complementation and genetic linkage between vaccinia virus temperature-sensitive mutants. Virology **119:**372–381.
12. **Duncan, S. A., and G. L. Smith.** 1992. Identification and characterization of an extracellular envelope glycoprotein affecting vaccinia virus egress. J. Virol. **66:**1610–1621.
13. **Dyster, L. M., and E. G. Niles.** 1991. Genetic and biochemical characterization of vaccinia virus genes D2L and D3R which encode virion structural proteins. Virology **182:**455–467.
14. **Ensinger, M. J.** 1982. Isolation and genetic characterization of temperature-sensitive mutants of vaccinia virus WR. J. Virol. **43:**778–790.
15. **Essani, K., R. Dugre, and S. Dales.** 1982. Biogenesis of vaccinia: involvement of spicules of the envelope during virion assembly examined by means of conditional lethal mutants and serology. Virology **118:**279–292.
16. **Fathi, Z., and R. C. Condit.** 1991. Phenotypic characterization of a vaccinia virus temperature-sensitive complementation group affecting a virion component. Virology **181:**273–276.
17. **Garcia-Beato, R., J. Freije, C. Lopez-Otin, R. Blasco, E. Vinuela, and M. L. Salas.** 1992. A gene homologous to topoisomerase II in African swine fever virus. Virology **188:**938–947.
18. **Gasser, S. M., and U. K. Laemmli.** 1986. Cohabitation of scaffold binding regions with upstream/enhancer elements of three developmentally regulated genes of D. melanogaster. Cell **46:**521–530.
19. **Giaever, G., R. Lynn, T. Goto, and J. C. Wang.** 1986. The complete nucleotide sequence of the structural gene TOP2 of yeast DNA topoisomerase II. J. Biol. Chem. **261:**12448–12454.
20. **Goebel, S. J., G. P. Johnson, M. E. Perkus, S. W. Davis, J. P. Winslow, and E. Paoletti.** 1990. The complete sequence of vaccinia virus. Virology **179:**247–266.
21. **Hall, R. L., and R. W. Moyer.** 1991. Identification, cloning, and sequencing of a fragment of *Amsacta moorei* entomopoxvirus DNA containing the spheroidin gene and three vaccinia virus-related open reading frames. J. Virol. **65:**6516–6527.
22. **Ichihashi, Y., M. Oie, and T. Tsuruhara.** 1984. Location of DNA-binding proteins and disulfide-linked proteins in vaccinia virus structural elements. J. Virol. **50:**929–938.
23. **Kane, E. M., and S. Shuman.** 1992. Temperature-sensitive mutations in the vaccinia virus H4 gene encoding a component of the virion RNA polymerase. J. Virol. **66:**5752–5762.
24. **Kao, S., E. Ressner, J. Kates, and W. R. Bauer.** 1981. Purification and characterization of a superhelix binding protein from vaccinia virus. Virology **111:**500–508.
25. **Miner, J. N., and D. E. Hruby.** 1989. Rifampin prevents virosome localization of L65, an essential vaccinia virus polypeptide. Virology **170:**227–237.
26. **Morgan, C.** 1976. Vaccinia virus reexamined: development and release. Virology **73:**43–58.
27. **Moriya, S., N. Ogasawara, and H. Yoshikawa.** 1985. Structure and function of the region of the replication origin of the *Bacillus subtilis* chromosome: nucleotide sequence of some 10,000 base pairs in the origin region. Nucleic Acids Res. **13:**2251–2265.

28. **Moss, B.** 1990. Replication of poxviruses, p. 2079–2112. *In* B. N. Fields, D. M. Knipe, R. M. Chanock, M. S. Hirsch, J. Melnick, T. P. Monath, and B. Roizman (ed.), Virology. Raven Press, New York.
29. **Niles, E. G., R. Condit, P. Caro, K. Davidson, L. Matusick, and J. Seto.** 1986. Nucleotide sequence and genetic map of the 16-kb vaccinia virus HindIII D fragment. Virology **153:**96–112.
30. **Perkus, M. E., K. Limbach, and E. Paoletti.** 1989. Cloning and expression of foreign genes in vaccinia virus, using a host range selection system. J. Virol. **63:**3829–3836.
31. **Rempel, R. E., and P. Traktman.** 1992. Vaccinia virus B1 kinase: phenotypic analysis of temperature-sensitive mutants and enzymatic characterization of recombinant proteins. J. Virol. **66:**4413–4426.
32. **Rodriguez, J. F., and G. L. Smith.** 1990. IPTG-dependent vaccinia virus: identification of a virus protein enabling virion envelopment by Golgi membrane and egress. Nucleic Acids Res. **18:**5347–5351.
33. **Rosel, J. L., P. L. Earl, J. P. Weir, and B. Moss.** 1986. Conserved TAAATG sequence at the transcriptional and translational initiation sites of vaccinia virus late genes deduced by structural and functional analysis of the *Hin*dIII H genome fragment. J. Virol. **60:**436–449.
34. **Rosenberg, A. H., B. N. Lade, D. Chui, S. Lin, J. J. Dunn, and F. W. Studier.** 1987. Vectors for selective expression of cloned DNAs by T7 RNA polymerase. Gene **56:**125–135.
35. **Schmitt, J., and H. G. Stunnenberg.** 1988. Sequence and transcriptional analysis of the vaccinia virus *Hin*dIII I fragment. J. Virol. **62:**1889–1897.
36. **Schmutz, C., L. G. Payne, J. Gubser, and R. Wittek.** 1991. A mutation in the gene encoding the vaccinia virus 37,000-M_r protein confers resistance to an inhibitor of virus envelopment and release. J. Virol. **65:**3435–3442.
37. **Seto, J., L. M. Celenza, R. C. Condit, and E. G. Niles.** 1987. Genetic map of the vaccinia virus *Hin*dIII D fragment. Virology **160:**110–119.
38. **Shuman, S.** 1992. Vaccinia virus RNA helicase: an essential enzyme related to the DE-H family of RNA-dependent NTPases. Proc. Natl. Acad. Sci. USA **89:**10935–10939.
39. **Shuman, S., S. S. Broyles, and B. Moss.** 1987. Purification and characterization of a transcription termination factor from vaccinia virions. J. Biol. Chem. **262:**12372–12380.
40. **Shuman, S., M. Golder, and B. Moss.** 1988. Characterization of vaccinia virus DNA topoisomerase I expressed in *Escherichia coli*. J. Biol. Chem. **263:**16401–16407.
41. **Shuman, S., M. Golder, and B. Moss.** 1988. Insertional mutagenesis of the vaccinia virus gene encoding a type I DNA topoisomerase: evidence that the gene is essential for virus growth. Virology **170:**302–306.
42. **Shuman, S., and B. Moss.** 1987. Identification of a vaccinia virus gene encoding a type I DNA topoisomerase. Proc. Natl. Acad. Sci. USA **89:**7478–7482.
43. **Tartaglia, J., and E. Paoletti.** 1985. Physical mapping and DNA sequence analysis of the rifampin resistance locus in vaccinia virus. Virology **147:**394–404.
44. **Thompson, C. L., and R. C. Condit.** 1986. Marker rescue mapping of vaccinia virus temperature-sensitive mutants using overlapping cosmid clones representing the entire virus genome. Virology **150:**10–20.
45. **Yang, W., and W. R. Bauer.** 1988. Purification and characterization of vaccinia virus structural protein VP8. Virology **167:** 578–584.
46. **Zhang, Y., and B. Moss.** 1991. Inducer-dependent conditional-lethal mutant animal viruses. Proc. Natl. Acad. Sci. USA **88:**1511–1515.
47. **Zhang, Y., and B. Moss.** 1991. Vaccinia virus morphogenesis is interrupted when expression of the gene encoding an 11-kilodalton phosphorylated protein is prevented by the *Escherichia coli lac* repressor. J. Virol. **65:**6101–6110.
48. **Zhang, Y., and B. Moss.** 1992. Immature viral particle formation is interrupted at the same stage by lac operator-mediated repression of the vaccinia virus D13L gene and by the drug rifampin. Virology **187:**643–653.